Eur. Phys. J. C (2009) 61: 429–438
DOI 10.1140/epjc/s10052-009-0989-z

THE EUROPEAN PHYSICAL JOURNAL C

Regular Article - Theoretical Physics

Hadronic B decays in the MSSM with large $\tan\beta$

M. Beneke[1,2,a], **Xin-Qiang Li**[1,b], **L. Vernazza**[1]

[1] Institut für Theoretische Physik E, RWTH Aachen University, 52056 Aachen, Germany
[2] Theory Division, CERN, 1211 Genève, Switzerland

Received: 6 February 2009 / Published online: 8 April 2009

Abstract We present an analysis of non-leptonic B decays in the minimally flavour-violating MSSM with large $\tan\beta$. We relate the Wilson coefficients of the relevant hadronic scalar operators to leptonic observables, showing that the present limits on the $B_s \to \mu^+\mu^-$ and $B^+ \to \tau^+\nu_\tau$ branching fractions exclude any visible effect in hadronic decays. We study the transverse helicity amplitudes of $B \to VV$ decays, which exhibit an enhanced sensitivity to the scalar operators, showing that even though an order one modification relative to the SM is not excluded in some of these amplitudes, they are too small to be detected at B factories.

1 Introduction

If new particles exist at the TeV scale, then the striking absence of evidence so far for their virtual effects in B or K meson mixing and decay suggests that the pattern of flavour-changing interactions is governed by the standard-model (SM) Yukawa coupling matrices even at the TeV scale. The minimal supersymmetric SM (MSSM) with large ratio $\tan\beta$ of the Higgs vacuum expectation values and no new sources of flavour violation in the supersymmetry-breaking Lagrangian is an example of such a minimally flavour-violating (MFV) theory, which nevertheless may exhibit sizeable differences from the SM due to Higgs exchange. The leptonic $B_s \to \mu^+\mu^-$ and $B^+ \to \tau^+\nu_\tau$ decays have been extensively studied in this model, as well as meson mixing and $B \to D\tau\nu_\tau$ [1–13]. Higgs exchange also generates scalar four-quark operators, which contribute to non-leptonic B decays. The effects of scalar operators on non-leptonic B decays have been studied in the MSSM (not necessarily minimally flavour-violating) and a general two Higgs doublet model in [14–21], mostly in connection with transverse polarization in B decays to two vector mesons (VV), and for specific decay modes. Some of these studies find large deviations from SM expectations for non-leptonic decays.

The present work is motivated by the question whether, given the present strong constraints from the leptonic decays, further insight on the MFV MSSM at large $\tan\beta$ can be derived from charmless non-leptonic B decays. To this end, extending previous analyses, we relate directly the Wilson coefficients of the leptonic to the relevant hadronic scalar operators, including charged Higgs exchange effects, and calculate the hadronic matrix elements in QCD factorization [22–24]. We also study observables related to the helicity amplitudes of $B \to VV$, which exhibit an enhanced sensitivity to the Higgs-induced scalar operators. We find that the present limit on the $B_s \to \mu^+\mu^-$ branching fraction, and the observation of $B^+ \to \tau^+\nu_\tau$ with a branching fraction close to the SM expectation, exclude any visible effects in hadronic decays, but for an academic exception: the positive-helicity amplitude of $\bar{B} \to VV$ modes may receive order one modifications relative to the SM. However, this amplitude is too small to be detected at present or planned B factories.

2 Scalar four-quark operators in the MSSM with large $\tan\beta$

In the SM the effective Hamiltonian for charmless B decays is

$$\mathcal{H}_{\rm eff}^{\rm SM} = \frac{G_F}{\sqrt{2}} \sum_{p=u,c} \lambda_p^{(D)} \Bigg(C_1 Q_1^p + C_2 Q_2^p + \sum_{i=3}^{10} C_i Q_i + C_{7\gamma} Q_{7\gamma} + C_{8g} Q_{8g} \Bigg) + \text{h.c.}, \tag{1}$$

where $D = d$ or s depending on the decay mode considered, and $\lambda_p^{(D)} = V_{pb} V_{pD}^*$ denotes a product of CKM matrix

[a] e-mail: mbeneke@physik.rwth-aachen.de

[b] X.-Q. Li is a Alexander-von-Humboldt fellow.

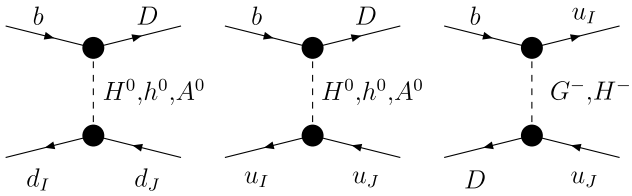

Fig. 1 Four-quark interactions mediated by neutral and charged Higgs bosons

elements. The conventions for the operators Q_i and the approximations for the short-distance coefficients C_i are given in [24]. Here we only note that the four-quark "current–current" and "penguin" operators $Q^p_{1,2}$, Q_{3-10} are all of the $(V-A)\times(V\mp A)$ form.

In the MSSM new four-quark operators are generated and the coefficients of the SM operators are modified. We consider the large-tan β scenario in a set-up, where the superpartner particles are somewhat heavier than the electroweak gauge bosons and the Higgs bosons (the "decoupling limit"), such that the leading effect is due to Higgs exchange not only for the neutral but also for the charged current interactions, as shown in Fig. 1. Of particular interest are the flavour-changing neutral Higgs couplings to fermions, which originate from a loop-induced coupling of the "wrong" Higgs field H_u to the down-type quarks, since these couplings are enhanced by several powers of $\tan\beta$ [2, 8, 10]. In the following we use the effective couplings given in [8, 10] in the decoupling limit to obtain the short-distance coefficients of the scalar four-quark operators from tree-level Higgs exchange. The coefficients are then evolved from the electroweak scale to the bottom mass scale m_b by the renormalization group equations. The relevant Higgs-induced terms in the effective Hamiltonian can be written as

$$\mathcal{H}^{\text{Higgs}}_{\text{eff}} = \frac{G_F}{\sqrt{2}} \sum_{p=u,c} \lambda_p^{(D)} \times \left(C^D_{11} Q^p_{11} + C^D_{12} Q^p_{12} + \sum_{i=13}^{14} \sum_{q=d,s,b} C^q_i Q^q_i \right) + \text{h.c.}, \tag{2}$$

similar to (1). The "current–current" operators

$$Q^p_{11} = (\bar p_i b_i)_{S+P} \big(\bar D_j p_j\big)_{S-P}, \quad Q^p_{12} = (\bar p_i b_j)_{S+P} \big(\bar D_j p_i\big)_{S-P}, \quad (p = u, c) \tag{3}$$

originate from charged Higgs exchange; the "penguin" operators

$$Q^q_{13} = \big(\bar D_i b_i\big)_{S+P} (\bar q_j q_j)_{S-P}, \quad Q^q_{14} = \big(\bar D_i b_j\big)_{S+P} (\bar q_j q_i)_{S-P}, \quad (q = d, s, b) \tag{4}$$

from the loop-induced neutral Higgs-fermion vertices. Here i, j denote colour indices and $(\bar q q)_{S\pm P} = \bar q\,(1 \pm \gamma_5) q$. The CKM factors $\lambda_p^{(D)}$ in (1), (2) are now assumed to be composed of the effective CKM matrix elements V^{eff}_{ij} that correspond to the low-energy couplings.

Neutral Higgs exchange: $b \to D\bar q q$ transitions

It is straightforward to assemble the short-distance coefficients from tree-level Higgs exchange in terms of the effective neutral Higgs couplings given in [8, 10]. Combining a flavour-changing and a flavour-conserving coupling, we find in the large-tan β limit, where $\sin\beta \approx 1$, $1/\cos\beta \approx \tan\beta$:

$$C^{d_J}_{13}(\mu_H) = \frac{1}{2} \frac{\bar m_{d_J} \bar m_b \epsilon_Y y_t^2 \tan^3\beta}{(1+\tilde\epsilon_3 \tan\beta)(1+\epsilon_0\tan\beta)(1+\tilde\epsilon_J \tan\beta)} \mathcal{F}^-_{2,J}, \tag{5}$$

$$C^{d_J}_{14}(\mu_H) = 0.$$

Here

$$\mathcal{F}^-_{2,J} = \frac{s_{\alpha-\beta}(c_\alpha + \tilde\epsilon_J s_\alpha)}{M^2_{H^0}} + \frac{c_{\alpha-\beta}(-s_\alpha + \tilde\epsilon_J c_\alpha)}{M^2_{h^0}} - \frac{1}{M^2_{A^0}} \approx -\frac{2}{M^2_{A^0}}, \tag{6}$$

with $c_\alpha \equiv \cos\alpha, \ldots$. The ϵ-coefficients appearing in (5) are defined in [10] and denote the loop-induced Higgs-fermion couplings. In the large-tan β MSSM products $\epsilon \times \tan\beta$ can be of order one. Just as in the $b \to D\ell_J\ell_J$ transitions, the coefficients of the hadronic Higgs penguin operators are strongly enhanced by the factor $\tan^3\beta$. The quark masses $\bar m_q$ are the $\overline{\text{MS}}$ masses in the low-energy effective theory at the matching scale μ_H.

Higgs exchange generates $(\bar D b)_{S-P}\,(\bar q q)_{S+P}$ operators as well, but in this case the factor $\bar m_b$ in (5) is replaced by $\bar m_D$, which is at most $\bar m_s$. The remaining two helicity combinations have short-distance coefficients multiplied by a function $\mathcal{F}^+_{2,J}$, which vanishes in the large-tan β limit. Thus, it is sufficient to consider the operators $Q^q_{13,14}$. The neutral Higgs coupling to up-type quarks (second diagram in Fig. 1) is suppressed at large tan β relative to the down-type quarks, thus $q = d_J = d, s, b$. In fact, the operators $Q^d_{13,14}$ might also be dropped due to the small down-quark mass. The operator $Q^b_{13,14}$ has the largest coefficient, but it contributes

to non-leptonic decays only through loops. Finally, we note that the double Higgs penguin diagrams (first diagram in Fig. 1 with flavour change at both vertices) are irrelevant to non-leptonic decays due to their extra CKM suppression. We therefore conclude that in the MFV MSSM with large $\tan\beta$, only a small set of scalar penguin operators $Q^{s,b}_{13,14}$ is relevant. Of these $Q^{s,b}_{14}$ is absent at tree level, but it is kept for the moment, since it may be generated by renormalization group evolution (see discussion below).

Charged Higgs exchange

The operators $Q^{p}_{11,12}$ arise from the third diagram in Fig. 1. Once again only the $(S+P)\times(S-P)$ Dirac structure is dominant at large $\tan\beta$. For charmless decays we need only the cases $u_I = u_J = p = u, c$, and obtain

$$C^D_{11}(\mu_H) = -\frac{\bar{m}_b \bar{m}_D}{M^2_{H^+}} \frac{\tan^2\beta}{(1+\epsilon_0\tan\beta)^2}, \qquad C^D_{12}(\mu_H) = 0. \tag{7}$$

Although C^D_{11} is enhanced only by $\tan^2\beta$, there is no loop suppression factor ϵ_Y. Due to the factor $\bar{m}_D$, charged Higgs exchange is relevant in practice only for $b \to s$ transitions.

Renormalization group evolution

We first discuss the evolution of the short-distance coefficients from a typical Higgs mass scale, which we assume to be $\mu_H = 200$ GeV, to the bottom mass scale $m_b = 4.2$ GeV, when penguin diagrams are neglected. Then each pair of operators (Q^p_{11}, Q^p_{12}), (Q^q_{13}, Q^q_{14}) evolves independently in leading logarithmic (LL) accuracy with anomalous dimension matrix (in units of $\alpha_s/(4\pi)$)

$$\gamma_{2\times2} = \begin{pmatrix} -16 & 0 \\ -6 & 2 \end{pmatrix}. \tag{8}$$

With $\alpha_s(m_b)/\alpha_s(\mu_H) \approx 2.13$, this results in

$$C^D_{11}(m_b)/C^D_{11}(\mu_H) = C^q_{13}(m_b)/C^q_{13}(\mu_H) \approx 2.20, \tag{9}$$

while $C^D_{12}(\mu)$, $C^q_{14}(\mu)$ remain zero. Using the 2-loop NDR scheme anomalous dimension matrix (ADM) [25] we obtain 2.35 instead and $C^D_{12}(m_b)/C^D_{11}(\mu_H) = C^q_{14}(m_b)/C^q_{13}(\mu_H) \approx 0.088$, but since we do not have the 1-loop correction to the initial condition of the scalar operators at μ_H, the next-to-leading logarithmic (NLL) evolution is not fully consistent. In any case, we conclude that the operators Q^p_{12}, Q^q_{14} can be neglected to first approximation, since their coefficient functions are suppressed by a factor 25.

Including penguin diagrams requires to enlarge the operator basis, since the scalar operators mix at the LL level into the SM penguin operators as well as their "mirror" copies, defined by a global exchange of left- and right chiralities of the quark fields. For the following discussion we neglect the electroweak penguin and magnetic dipole operators, so we deal with the six SM operators $Q^p_{1,2}$, Q_{3-6}, their mirror copies $Q'^p_{1,2}$, Q'_{3-6}, and the six scalar operators $Q^p_{11,12}$, $Q^{D,b}_{13,14}$. The structure of the ADM reads

$$\gamma = \begin{pmatrix} \gamma_{6\times6} & 0_{6\times6} & 0_{6\times6} \\ 0_{6\times6} & \gamma'_{6\times6} & 0_{6\times6} \\ \gamma^{\mathrm{sc-p}}_{6\times6} & \gamma'^{\mathrm{sc-p}}_{6\times6} & \gamma^{\mathrm{sc}}_{6\times6} \end{pmatrix}, \tag{10}$$

where $\gamma_{6\times6} = \gamma'_{6\times6}$ is the ADM for the SM current–current and QCD penguin operators (equal for the mirror operators) and $\gamma^{\mathrm{sc}}_{6\times6}$ is a block-diagonal matrix with three identical 2×2 blocks given by $\gamma_{2\times2}$ in (8): one for $Q^p_{11,12}$, one for $Q^D_{13,14}$, depending on the transition, and one for $Q^b_{13,14}$. The matrices $\gamma^{(\prime)\,\mathrm{sc-p}}_{6\times6}$ describe the mixing of the scalar operators into the penguin operators. We find that $Q^p_{11,12}$ and $Q^D_{13,14}$ mix into the mirror penguin operators, while only $Q^b_{13,14}$ mixes into the SM penguins. Thus $[\gamma^{\mathrm{sc-p}}_{6\times6}]^T = (0|0|\Gamma^T)$ and $[\gamma'^{\mathrm{sc-p}}_{6\times6}]^T = (\Gamma^T|\Gamma^T|0)$, where

$$\Gamma = \begin{pmatrix} 0 & 0 & \frac{1}{9} & -\frac{1}{3} & \frac{1}{9} & -\frac{1}{3} \\ 0 & 0 & 0 & 0 & 0 & 0 \end{pmatrix}. \tag{11}$$

Solving the RGE equations leaves (9) unchanged, generates the mirror QCD penguin operators with coefficient functions

$$C'^D_i(m_b) \approx -0.71 C^{\mathrm{SM}}_i(m_b) \times \left[C^D_{11}(\mu_H) + C^D_{13}(\mu_H)\right], \quad i = 3,\ldots,6, \tag{12}$$

and modifies the SM penguin coefficients according to $C_i = C^{\mathrm{SM}}_i + \delta C_i$ with

$$\delta C_i(m_b) \approx -0.71 C^{\mathrm{SM}}_i(m_b) \times C^b_{13}(\mu_H), \quad i = 3,\ldots,6. \tag{13}$$

Since the SM penguin coefficients $C^{\mathrm{SM}}_i(m_b)$ are small numbers, the penguin-mixing effects are small, unless the coefficient functions of the scalar operators are of order one. However, due to their different chiral structure, the mirror penguin operators contribute differently from the standard ones to the transverse helicity amplitudes in $B \to VV$ decays as discussed below.

3 Constraints from $B_s \to \mu^+\mu^-$ and $B^+ \to \tau^+\nu_\tau$

The natural size of the loop-induced neutral Higgs couplings $\epsilon_0, \epsilon_Y, \tilde{\epsilon}_J$ is of order 0.01, the precise values depending on MSSM parameters. Assuming $M_{A^0} = 200$ GeV

and $\tan\beta = 50$, this allows the scalar penguin operators to have coefficients of order $C_{13}^{s} \simeq 0.01$, $C_{13}^{b} \simeq 0.5$, which are comparable to SM penguin coefficients. However, the non-observation of $B_s \to \mu^+\mu^-$ implies much stronger limits on the size of the scalar four-quark operator coefficient functions.

The decay $B_s \to \mu^+\mu^-$ proceeds via an interaction similar to the first diagram of Fig. 1 except that the lower legs are replaced by a muon pair. Since the lower vertex is a tree-level neutral Higgs coupling, the leptonic and hadronic decay are closely related. For large $\tan\beta$, a single scalar operator $(\bar{D}b)_{S+P}(\bar{\mu}\mu)_{S-P}$, similar in structure to Q_{13}^{q}, dominates the $B_s \to \mu^+\mu^-$ decay amplitude. Its coefficient function is given by

$$C_{\mu\mu}(\mu_H) = -\frac{1}{2}\frac{\bar{m}_b m_\mu \epsilon_Y y_t^2 \tan^3\beta}{(1+\tilde{\epsilon}_3\tan\beta)(1+\epsilon_0\tan\beta)}\mathcal{F}_{2l}^{-}, \tag{14}$$

with

$$\mathcal{F}_{2l}^{-} = \frac{s_{\alpha-\beta}(c_\alpha)}{M_{H_0}^2} + \frac{c_{\alpha-\beta}(-s_\alpha)}{M_{h_0}^2} - \frac{1}{M_{A_0}^2} \approx \mathcal{F}_{2,J}^{-}. \tag{15}$$

For large $\tan\beta$, and at the level of the present experimental limit, the SM contribution to the decay amplitude is negligible, and the branching ratio is given by

$$\mathrm{Br}\big(B_s \to \mu^+\mu^-\big) = \frac{G_F^2 f_{B_s}^2 m_{B_s}^5 \tau_{B_s}}{8\pi(\bar{m}_b+\bar{m}_s)^2}\big|\lambda_t^{(s)}\big|^2 |C_{\mu\mu}|^2. \tag{16}$$

Comparing (5) to (14), we see that we can eliminate $C_{\mu\mu}$ in favour of C_{13}^{q} in the previous equation and turn it into

$$\begin{aligned}(1+\tilde{\epsilon}_J\tan\beta)\big|C_{13}^{d_J}(\mu_H)\big| &= \frac{2\sqrt{2\pi}(\bar{m}_b+\bar{m}_s)(\mu_H)}{G_F f_{B_s} m_{B_s}^{5/2}\tau_{B_s}^{1/2}|\lambda_t^{(s)}|}\frac{\bar{m}_{d_J}(\mu_H)}{m_\mu} \\ &\quad\times\big[\mathrm{Br}(B_s\to\mu^+\mu^-)\big]^{1/2}.\end{aligned} \tag{17}$$

The present experimental upper limit on the $B_s \to \mu^+\mu^-$ branching fraction is $\mathrm{Br}(B_s \to \mu^+\mu^-) \le 5.8 \times 10^{-8}$ at 95% C.L. [26]. Using $f_{B_s} = 240$ MeV, $\bar{m}_s(2\ \mathrm{GeV}) = 90$ MeV and $\bar{m}_b(\bar{m}_b) = 4.2$ GeV, and evolving both quark masses to the common scale $\mu_H = 200$ GeV, we obtain

$$\begin{aligned}(1+\epsilon_0\tan\beta)\big|C_{13}^{s}(\mu_H)\big| &\le 1.4\times10^{-4}, \\ (1+\tilde{\epsilon}_3\tan\beta)\big|C_{13}^{b}(\mu_H)\big| &\le 7.9\times10^{-3}.\end{aligned} \tag{18}$$

When ϵ_0 and/or $\tilde{\epsilon}_3$ are negative, the coefficient functions can be larger than the values on the right-hand side. However, the brackets multiplying the coefficient functions enter the relation between the quark masses and the down-type Yukawa couplings, and hence $(1+\tilde{\epsilon}_3\tan\beta)$ cannot become very small, if the bottom Yukawa coupling is to remain perturbative. We allow a factor of three enhancement of the coefficient functions to be conservative (that is, the brackets are required to be larger than 1/3). Including the factor (9) from evolution to the scale m_b leads to

$$\big|C_{13}^{s}(m_b)\big| \le 0.001, \qquad \big|C_{13}^{b}(m_b)\big| \le 0.05, \tag{19}$$

while $C_{13}^{d}(m_b)$ is a factor $\bar{m}_d/\bar{m}_s$ smaller than $C_{13}^{s}(m_b)$ and therefore negligible. Thus, the coefficient functions of the hadronic flavour-changing neutral Higgs penguin operators are constrained to be a factor of 10 smaller than the above estimates derived from $M_{A^0} = 200$ GeV and $\tan\beta = 50$.

The short-distance coefficient $C_{11}^{D}(\mu_H)$, arising from charged Higgs exchange, can be related to $B^+ \to \tau^+\nu_\tau$ in a similar way. Using (7) the ratio [11, 27]

$$\begin{aligned}R_{\tau\nu_\tau} &\equiv \frac{\mathrm{Br}(B^+\to\tau^+\nu_\tau)_{\mathrm{MSSM}}}{\mathrm{Br}(B^+\to\tau^+\nu_\tau)_{\mathrm{SM}}} \\ &= \left(1 - \frac{m_B^2}{m_{H^+}^2}\frac{\tan^2\beta}{1+\epsilon_0\tan\beta}\right)^2\end{aligned} \tag{20}$$

is expressed in terms of $C_{11}^{D}(\mu_H)$ as

$$R_{\tau\nu_\tau} = \left(1 + C_{11}^{D}(\mu_H)\frac{m_B^2(1+\epsilon_0\tan\beta)}{\bar{m}_D(\mu_H)\bar{m}_b(\mu_H)}\right)^2. \tag{21}$$

The present average of the Babar and Belle measurements of the branching fraction is $\mathrm{Br}(B^+\to\tau^+\nu_\tau) = (1.51\pm0.33)\times 10^{-4}$ [28–30]. Employing the central value $|V_{ub}|\, f_{B_d} = 7.4\times10^{-4}$ GeV and assigning a conservative 50% uncertainty to the SM prediction of the branching fraction, the measurement constrains $R_{\tau\nu_\tau}$ to lie in the range

$$0.72 < R_{\tau\nu_\tau} < 2.40. \tag{22}$$

Concentrating on the case $D = s$ this implies the allowed ranges

$$\begin{aligned}-0.012 &< (1+\epsilon_0\tan\beta)\, C_{11}^{s}(\mu_H) < -0.009, \\ -0.001 &< (1+\epsilon_0\tan\beta)\, C_{11}^{s}(\mu_H) < 0.003.\end{aligned} \tag{23}$$

The first range corresponds to the situation, where the charged Higgs contribution is about twice as large as the SM one, and opposite in sign. Requiring $1+\epsilon_0\tan\beta > 1/3$ and including the RG evolution (9) results in

$$\begin{aligned}-0.08 &< C_{11}^{s}(m_b) < -0.06, \quad \text{or} \\ -0.005 &< C_{11}^{s}(m_b) < 0.018.\end{aligned} \tag{24}$$

The constraint from $B^+ \to \tau^+\nu_\tau$ on C_{11}^{s} is not as stringent as the one from $B_s \to \mu^+\mu^-$ on C_{13}^{s}, but one must remember that the charged Higgs contribution to hadronic charmless decays must compete with the SM tree operators rather

than the penguin operators. In addition, since $|C_{11}^s| \ll 1$, the contribution (12) to the mirror penguin coefficients remains small. These conclusions hold a fortiori for C_{11}^d, which is a factor of $\bar{m}_d/\bar{m}_s$ smaller than C_{11}^s.

To conclude this section, we remark that we also performed a MSSM parameter space scan, calculating explicitly the loop-induced ϵ parameters subject to the experimental constraints from $B_s \to \mu^+\mu^-$, $B^+ \to \tau^+\nu_\tau$, $B \to X_s\gamma$, and $\Delta M_{B_{d,s}}$. Here we also included the subleading scalar operators for $B_s \to \mu^+\mu^-$, as well as the exact expressions for $\mathcal{F}_{2,J}^-$, $\mathcal{F}_{2l}^-$ and related functions. The resulting values of the short-distance coefficients C_{11}^D, C_{13}^q are in agreement with the ranges given above.

4 Hadronic matrix elements for $B \to M_1M_2$

To calculate the decay amplitudes of non-leptonic, charmless B decays, we employ the QCD factorization (QCDF) framework [22–24]. We refer to these papers for a discussion of the method and to [31, 32] for the definitions and notation that we adopt below. Let us emphasize that given the constraints on the coefficient functions, a leading-order treatment, where QCDF is equivalent to naive factorization [33], would suffice. However, it takes little additional effort to include the first-order radiative corrections.

The matrix element of the effective Hamiltonian is written as

$$\langle M_1'M_2'|\mathcal{H}_{\rm eff}|\bar{B}\rangle = \sum_{p=u,c} \lambda_p^{(D)} \langle M_1'M_2'|\mathcal{T}_A^p + \mathcal{T}_B^p|\bar{B}\rangle, \qquad (25)$$

where $\mathcal{T}_A^p$ account for vertex, penguin and spectator-scattering terms in the QCDF formula and $\mathcal{T}_B^p$ parameterizes the weak annihilation amplitudes. We generalize the expression given in [31] to account for the scalar amplitudes and those from the mirror QCD penguin operators, such that now

$$\begin{aligned}
\mathcal{T}_A^p &= \delta_{pu}\big[\alpha_1(M_1M_2) + \alpha_{11}^D(M_1M_2)\big]A\big([\bar{q}_s u][\bar{u}D]\big) \\
&\quad + \delta_{pu}\big[\alpha_2(M_1M_2) + \alpha_{12}^D(M_1M_2)\big]A\big([\bar{q}_s D][\bar{u}u]\big) \\
&\quad + \big[\alpha_3^p(M_1M_2) + \alpha_3'^{pD}(M_1M_2)\big] \\
&\quad \times \sum_{q=u,d,s} A\big([\bar{q}_s D][\bar{q}q]\big) \\
&\quad + \big[\alpha_4^p(M_1M_2) + \alpha_4'^{pD}(M_1M_2)\big] \\
&\quad \times \sum_{q=u,d,s} A\big([\bar{q}_s q][\bar{q}D]\big) \\
&\quad + \alpha_{3,\rm EW}^p(M_1M_2) \sum_{q=u,d,s} \frac{3}{2}e_q A\big([\bar{q}_s D][\bar{q}q]\big) \\
&\quad + \alpha_{4,\rm EW}^p(M_1M_2) \sum_{q=u,d,s} \frac{3}{2}e_q A\big([\bar{q}_s q][\bar{q}D]\big) \\
&\quad + \sum_{q=d,s} \alpha_{3q}^p(M_1M_2)A\big([\bar{q}_s D][\bar{q}q]\big) \\
&\quad + \sum_{q=d,s} \alpha_{4q}^p(M_1M_2)A\big([\bar{q}_s q][\bar{q}D]\big). \qquad (26)
\end{aligned}$$

The new contributions are encoded in $\alpha_{11,12}^D$ (charged Higgs effects), $\alpha_{3,4}'^{pD}$ (mirror QCD penguins) and $\alpha_{3q,4q}^p$ (neutral Higgs effects), as well as modifications of the standard QCD penguin amplitudes $\alpha_{3,4}^p$. A similar generalization applies to the annihilation amplitudes. Our aim is to compare the new coefficients to those present in the SM for PP, PV, VP, VV (P pseudoscalar, V vector meson) final states. Note that for VV, (25) and (26) apply separately to each of the three independent helicity amplitudes $h = 0, -, +$, but the helicity label is suppressed in our notation.

In (26) $A([\bar{q}_{M_1}q_{M_1}][\bar{q}_{M_2}q_{M_2}])$ refers to a product of decay constant, form factor and other factors [31, 32], and the arguments indicate the flavour content of the final state mesons M_1M_2. Since $V \pm A$ and $S \pm P$ operators contribute differently to pseudoscalar and vector final states we next write[1]

$$\begin{aligned}
&\alpha_3'^p(M_1M_2) \\
&= \begin{cases}
-a_3'^p(M_1M_2) + a_5'^p(M_1M_2), & \text{if } M_1M_2 = PP, \\
a_3'^p(M_1M_2) + a_5'^p(M_1M_2), & \text{if } M_1M_2 = PV, \\
a_3'^p(M_1M_2) - a_5'^p(M_1M_2), & \text{if } M_1M_2 = VP, \\
-a_3'^p(M_1M_2) - a_5'^p(M_1M_2), & \text{if } M_1M_2 = V^0V^0, \\
-f_\pm^{M_1}\big(a_3'^p(M_1M_2) + a_5'^p(M_1M_2)\big), & \text{if } M_1M_2 = V^\pm V^\pm,
\end{cases} \\
&\alpha_4'^p(M_1M_2) \\
&= \begin{cases}
-a_4'^p(M_1M_2) - r_\chi^{M_2}a_6'^p(M_1M_2), & \text{if } M_1M_2 = PP, \\
a_4'^p(M_1M_2) + r_\chi^{M_2}a_6'^p(M_1M_2), & \text{if } M_1M_2 = PV, \\
a_4'^p(M_1M_2) - r_\chi^{M_2}a_6'^p(M_1M_2), & \text{if } M_1M_2 = VP, \\
-a_4'^p(M_1M_2) + r_\chi^{M_2}a_6'^p(M_1M_2), & \text{if } M_1M_2 = V^0V^0, \\
f_\pm^{M_1}\big(-a_4'^p(M_1M_2) + r_\chi^{M_2}a_6'^p(M_1M_2)\big), & \text{if } M_1M_2 = V^\pm V^\pm,
\end{cases} \qquad (27) \\
&\alpha_{3q}^p(M_1M_2) \\
&= \frac{r_\chi^{M_2}}{2}\begin{cases}
a_{13q}^p(M_1M_2), & \text{if } M_1M_2 = PP, VP, \\
-a_{13q}^p(M_1M_2), & \text{if } M_1M_2 = PV, V^0V^0, \\
-f_\pm^{M_1}a_{13q}^p(M_1M_2), & \text{if } M_1M_2 = V^\pm V^\pm,
\end{cases} \\
&\alpha_{4q}^p(M_1M_2) \\
&= \frac{1}{2}\begin{cases}
-a_{14q}^p(M_1M_2), & \text{if } M_1M_2 = PP, PV, \\
a_{14q}^p(M_1M_2), & \text{if } M_1M_2 = VP, V^0V^0, \\
f_\pm^{M_1}a_{14q}^p(M_1M_2), & \text{if } M_1M_2 = V^\pm V^\pm;
\end{cases}
\end{aligned}$$

[1] In the following we drop the superscript "D" (referring to $b \to D$ transitions) on the amplitude parameters and Wilson coefficients of the mirror penguin contributions.

the same relations as the last two hold between α_{11}^D and a_{11D}, and between α_{12}^D and a_{12D}, respectively. We denote by $f_\pm^{M_1} = F_\mp^{B\to M_1}(0)/F_\pm^{B\to M_1}(0)$ a ratio of form factors, such that $f_+^{M_1} \sim m_B/\Lambda_{\rm QCD}$ and $f_-^{M_1} \sim \Lambda_{\rm QCD}/m_B$ in the heavy-quark limit [32]. It follows that for the transverse helicity amplitudes of $\bar B \to VV$ decay modes the contributions from the new operators obey a different hierarchy in the heavy-quark limit. While in the SM

$$\bar{\mathcal{A}}_0 : \bar{\mathcal{A}}_- : \bar{\mathcal{A}}_+ = 1 : \frac{\Lambda_{\rm QCD}}{m_b} : \frac{\Lambda_{\rm QCD}^2}{m_b^2} \tag{28}$$

(up to certain electromagnetic effects [34]), the Higgs contributions to the amplitude satisfy

$$\bar{\mathcal{A}}_0 : \bar{\mathcal{A}}_- : \bar{\mathcal{A}}_+ = 1 : \frac{\Lambda_{\rm QCD}^2}{m_b^2} : \frac{\Lambda_{\rm QCD}}{m_b}. \tag{29}$$

This effect, noted first in [17], is interesting, since it increases the sensitivity of certain polarization observables to the new short-distance coefficients by a factor $f_+^{M_1} \approx 10$. On the other hand, the absence of tensor operators implies that the formal dominance of the longitudinal amplitude is preserved by the Higgs contributions.

In QCDF the $a_{iq}^{(\prime)\,p}$ coefficients introduced in (27) can be written at next-to-leading order (NLO) in the form

$$\begin{aligned} a_{iq}^{(\prime)\,p}(M_1M_2) = {} & \left(C_i^{(\prime)\,q} + \frac{C_{i\pm1}^{(\prime)\,q}}{N_c}\right) N_i^{(\prime)}(M_2) \\ & + \frac{C_{i\pm1}^{(\prime)\,q}}{N_c}\frac{C_F\alpha_s}{4\pi} \\ & \times \left[V_i^{(\prime)}(M_2) + \frac{4\pi^2}{N_c} H_i^{(\prime)}(M_1M_2)\right] \\ & + P_i^{(\prime)\,p}(M_2), \end{aligned} \tag{30}$$

where the upper (lower) signs apply when i is odd (even). The quantities $N_i^{(\prime)}(M_2)$, $V_i^{(\prime)}(M_2)$, $H_i^{(\prime)}(M_1M_2)$, $P_i^{(\prime)\,p}(M_2)$ stand, respectively, for the tree-level result ("naive factorization"), the 1-loop vertex correction, spectator scattering, and the penguin diagrams.

The leading-order (naive factorization) term in (30) is simply a combination of short-distance coefficients, except for cases where a vector meson couples to a scalar current, where it is zero. This is summarized by

$$N_i^{(\prime)}(M_2) = \begin{cases} 1, & \text{for } i = 3,4,5,12,14q, \\ 1, & \text{for } i = 6,11,13q \text{ and } M_2 = P, \\ 0, & \text{for } i = 6,11,13q \text{ and } M_2 = V. \end{cases} \tag{31}$$

The NLO coefficients in (30) can mostly be expressed in terms of those already known from the SM operators [22–24, 31, 32]. For the mirror QCD penguin operators, we find that they are almost identical to the SM QCD penguins, that is $V_i'(M_2) = V_i(M_2)$, $H_i'(M_1M_2) = H_i(M_1M_2)$ for $i = 3,\ldots,6$. For the penguin contribution $P_{4,6}^{\prime\,p}(M_2)$ one replaces $C_i \to C_i'$ in the SM expression and then adds the term $\delta P_{4,6}^{\prime\,p}(M_2)$ from the scalar operators given in (36) below. For the scalar operators, we set C_{12}^D and C_{14}^q to zero (see Sect. 2) and, using the Fierz symmetry of the NDR renormalization scheme for the scalar operators [25], we obtain

$$\begin{aligned} & a_{11D}(M_1M_2) = C_{11}^D N_{11}, \\ & a_{12D}(M_1M_2) \\ & \quad = \frac{C_{11}^D}{N_c} + \frac{C_{11}^D}{N_c}\frac{C_F\alpha_s}{4\pi}\left[V_5(M_2) + \frac{4\pi^2}{N_c} H_5(M_1M_2)\right], \end{aligned} \tag{32}$$

$$\begin{aligned} & a_{13q}^p(M_1M_2) = C_{13}^q N_{13q}, \\ & a_{14q}^p(M_1M_2) \\ & \quad = \frac{C_{13}^q}{N_c} + \frac{C_{13}^q}{N_c}\frac{C_F\alpha_s}{4\pi}\left[V_5(M_2) + \frac{4\pi^2}{N_c} H_5(M_1M_2)\right], \end{aligned} \tag{33}$$

where $V_5(M_2)$, $H_5(M_1M_2)$ can be found in [31] for PP, PV, and VP final states and in [32] for VV. (Although not used in the following, since we set C_{12}^D and C_{14}^q to zero, we note that similarly $V_{11}(M_2) = V_{13}(M_2) = V_6(M_2)$, and $H_{11}(M_1M_2) = H_{13}(M_1M_2) = H_6(M_1M_2)$.)

There are no penguin contributions to (33). However, as discussed above, the insertion of scalar operators into the penguin diagrams shown in Fig. 2 modifies the evolution of the (mirror) QCD penguin operators. Accordingly, it also contributes to the penguin terms $P_{4,6}^{(\prime)\,p}(M_2)$ in $a_{4,6}^{(\prime)\,p}(M_1M_2)$. The correction terms are proportional to the coefficient functions of the scalar operators and read

$$\begin{aligned} & \delta P_4^p(M_1M_2) = \frac{C_F\alpha_s}{4\pi N_c}\left(-\frac{1}{2}\right) C_{13}^b \left[\frac{4}{3}\log\frac{m_b}{\mu} - G_{M_2}^f(1)\right], \\ & \delta P_6^p(M_1M_2) \\ & \quad = \frac{C_F\alpha_s}{4\pi N_c}\left(-\frac{1}{2}\right) C_{13}^b \left[N_6(M_2)\frac{4}{3}\log\frac{m_b}{\mu} - \hat G_{M_2}^f(1)\right], \end{aligned} \tag{34}$$

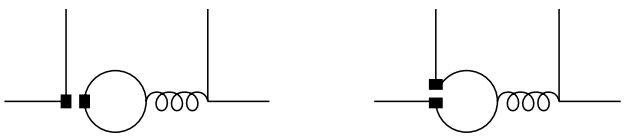

Fig. 2 Penguin contractions. Due to colour only the second diagram contributes to insertions of Q_{11}^p, Q_{13}^q

where $G^f_{M_2}(s)$ equals $G_{M_2}(s)$ [31] for $M_1M_2 = PP, PV$, VP, V^0V^0, and $G^\pm_{M_2}(s)$ [32] for $V^\pm V^\pm$ with

$$G^+_{V_2}(s) = \int_0^1 dy\, \phi_{a2}(y) G(s - i\epsilon, 1-y), \tag{35}$$

while $\hat{G}^f_{M_2}(s)$ equals $\hat{G}_{M_2}(s)$ for $M_1M_2 = PP, PV$, VP, V^0V^0, and is zero for $V^\pm V^\pm$. Similarly, for the mirror penguin coefficients

$$\begin{aligned}
\delta P'^p_4(M_1M_2) &= \frac{C_F\alpha_s}{4\pi N_c}\left(-\frac{1}{2}\right)\left\{C^D_{13}\left[\frac{4}{3}\log\frac{m_b}{\mu} - G^f_{M_2}(0)\right]\right. \\
&\quad \left. + C^D_{11}\left[\frac{4}{3}\log\frac{m_b}{\mu} - G^f_{M_2}(s_p)\right]\right\}, \\
\delta P'^p_6(M_1M_2) &= \frac{C_F\alpha_s}{4\pi N_c}\left(-\frac{1}{2}\right) \\
&\quad \times \left\{C^D_{13}\left[N_6(M_2)\frac{4}{3}\log\frac{m_b}{\mu} - \hat{G}^f_{M_2}(0)\right]\right. \\
&\quad \left. + C^D_{11}\left[N_6(M_2)\frac{4}{3}\log\frac{m_b}{\mu} - \hat{G}^f_{M_2}(s_p)\right]\right\},
\end{aligned} \tag{36}$$

where $s_u = 0$, $s_c = (m_c/m_b)^2$, and now $G^f_{M_2}(s)$ equals $G^\mp_{M_2}(s)$ for $V^\pm V^\pm$ and else as above. Note that the explicit scale dependence in $\delta P^{(\prime)p}_{4,6}(M_2)$ cancels the extra scale dependence of the (mirror) QCD penguin coefficients at LL accuracy. At this point we should mention that the constant terms in the real part of the NLO matrix elements should strictly speaking only be considered at the NLL order. At this order, our calculation is, however, incomplete, since we do not consider the 1-loop QCD correction to the initial condition of the scalar operators, and the 2-loop mixing into the penguin operators, as well as the small contributions from C^D_{12} and C^q_{14}. Since we do not need precise results for the NLO terms, as will be seen below, the present approximation is adequate for our purpose. However, the complete NLO results for the matrix elements of scalar and mirror penguin operators given above might be of more general interest.

We also calculated the weak annihilation terms $\mathcal{T}^p_B$ originating from the scalar operators. In some cases the annihilation amplitude can be as large as the corresponding α_i amplitude. Since no precise estimates are needed below, we do not discuss the annihilation amplitudes further.[2]

[2]We use this occasion to point out the following corrections to [32]: The overall sign on the right-hand side of (A.15) ((63) in the arXiv version) must be minus. Furthermore, the expression for $A^{i,0}_3$ [$A^{f,0}_3$] in (A.20) (eq. (68)) must contain $r^{V_1}_\chi - r^{V_2}_\chi$ [$r^{V_1}_\chi + r^{V_2}_\chi$] rather than the opposite relative sign [35]. (However, the unsimplified expressions in (A.18) (eq. (66)) are given correctly.)

5 Non-leptonic decays

We are now ready to discuss the question whether there are observable effects on non-leptonic, charmless decays due to Higgs exchange in the MSSM with large $\tan\beta$. To this end, we compare the new amplitudes to those present in the SM. The essential features can be deduced from (26).

- Charged Higgs exchange ($\alpha^D_{11,12}$) contributes directly to tree-dominated decays (such as $B \to \pi\pi, \pi\rho, \rho\rho$), but must compete with the sizeable SM tree amplitudes $\alpha_{1,2}$. However, since $\alpha^D_{11,12} \propto \bar{m}_D$, only the case of $b \to s\bar{u}u$ transitions is of interest. But there are no tree-dominated decays of this type, since for $D = s$ the tree amplitudes are doubly CKM-suppressed, $\lambda^{(s)}_u \ll \lambda^{(s)}_c$.
- The effects from the mirror QCD penguin operators ($\alpha'^p_{3,4}$) must compete with the SM penguin amplitudes, which according to (12) requires the scalar operator Wilson coefficients to be of order 1 in general, and of order 0.1 in case of the plus-helicity amplitude in $\bar{B} \to VV$.
- The direct contribution from the FCNC Higgs couplings ($\alpha^p_{3q,4q}$) is an isospin-violating effect that must compete only with the small SM electroweak penguins, and is therefore most likely to lead to an observable effect. Since $\alpha^p_{3q,4q} \propto \bar{m}_q$, only the case $q = s$ is of interest. For the case of $D = s$, the $b \to s\bar{s}s$ transition leads to final states with flavour content $M_1 = \bar{q}_s s$, $M_2 = \bar{s}s$ with $\bar{q}_s$ the flavour of the $\bar{B}$ meson spectator antiquark. This singles out the decay modes $\bar{B} \to \bar{K}^{(*)}(\eta^{(\prime)}, \phi)$ and $\bar{B}_s \to (\eta^{(\prime)}, \phi)(\eta^{(\prime)}, \phi)$. For the case of $D = d$, the potentially interesting modes are $\bar{B} \to \bar{K}^{(*)}K^{(*)}$ and $\bar{B}_s \to K^{(*)}\phi$. However, in all these decays it is impossible to extract the EW penguin amplitude, so the new contributions must in fact be compared to the larger SM QCD penguins.

We now proceed to a more detailed discussion. The numerical amplitude values given below depend on parameters (quark masses, form factors, etc.), for which we choose values as given in [31, 32], including some updates. Since none of our conclusions depends on the precise values of these parameters, we do not list them here. The Wilson coefficients are evaluated at the scale $\mu = m_b = 4.2$ GeV.

$B \to PP, PV$

In Table 1 we show the numerical results of the α_i amplitude coefficients defined in (26) for the decay modes $\bar{B} \to \bar{K}\eta, \bar{K}^*\eta, \bar{K}\phi$. ($\eta_s$ in the table refers to the strange component of η, see [36].) To evaluate the Higgs contributions we assume the largest values of the coefficient functions allowed by the constraints from leptonic decays derived in Sect. 3, in detail: $C^s_{11}(m_b) = -0.08$, $C^s_{13}(m_b) = 0.001$, $C^b_{13}(m_b) = 0.05$.

Table 1 Numerical results for the α_i coefficients of some representative $\Delta S = 1$ decay channels. The value of α_4^u corresponds to the SM contribution only. The final states $\bar{K}\eta_s$, $\bar{K}^*\eta_s$, $\bar{K}\phi$ do not receive tree-amplitude contributions. For $\alpha_{1,2}$ and $\alpha^s_{11,12}$, we therefore provide results for the final states in square brackets

	$\bar{K}\eta_s$	$\bar{K}^*\eta_s$	$\bar{K}\phi$
α_1	$0.966 + 0.021i$ $[\pi\bar{K}]$	$0.981 + 0.021i$ $[\rho\bar{K}]$	$0.973 + 0.021i$ $[\pi\bar{K}^*]$
α_2	$0.351 - 0.084i$ $[\bar{K}\pi]$	$0.260 - 0.084i$ $[\bar{K}^*\pi]$	$0.323 - 0.084i$ $[\bar{K}\rho]$
α^s_{11}	-0.059 $[\pi\bar{K}]$	-0.059 $[\rho\bar{K}]$	0 $[\pi\bar{K}^*]$
α^s_{12}	$0.003 + 0.003i$ $[\bar{K}\pi]$	$-0.006 - 0.003i$ $[\bar{K}^*\pi]$	$0.004 + 0.003i$ $[\bar{K}\rho]$
α^u_3	$-0.0013 + 0.0046i$	$0.0027 + 0.0046i$	$0.0006 - 0.0005i$
α^u_4	$-0.095 - 0.040i$	$0.038 + 0.008i$	$-0.031 - 0.017i$
δP^u_4	1.4×10^{-5}	1.4×10^{-5}	1.4×10^{-5}
δP^u_6	1.4×10^{-5}	1.4×10^{-5}	-1.5×10^{-5}
α'^u_3	$7.8 \times 10^{-5} - 0.0001i$	$2.8 \times 10^{-5} + 0.0001i$	$(1.4 - 1.3i) \times 10^{-5}$
α'^u_4	$0.0035 + 0.0015i$	$0.0011 + 0.0003i$	$-0.0013 - 0.0006i$
$\delta P'^u_4$	$-0.0005 - 0.0007i$	$-0.0005 - 0.0007i$	$-0.0005 - 0.0007i$
$\delta P'^u_6$	$-0.0006 - 0.0007i$	$-0.0006 - 0.0007i$	-0.0003
$\alpha^u_{3,\mathrm{EW}}$	$-0.0089 - 0.0002i$	$-0.0091 - 0.0002i$	$-0.0082 - 0.0001i$
$\alpha^u_{4,\mathrm{EW}}$	$-0.0016 + 0.0006i$	$-0.0025 + 0.0008i$	$-0.0024 + 0.0007i$
α^u_{3s}	0.00078	0.00078	0
α^u_{4s}	$(-6.3 - 3.7i) \times 10^{-5}$	$(9.7 + 3.7i) \times 10^{-5}$	$(-6.3 - 3.7i) \times 10^{-5}$

Table 2 Numerical results for the α_i coefficients pertaining to the three helicity amplitudes of $\bar{B} \to VV$ decays. The value of α^u_4 corresponds to the SM contribution only. To compare the absolute values of the helicity amplitudes the numbers for the $(00, --, ++)$ parameters must be multiplied by $A_{K^*\phi} = \frac{iG_F}{\sqrt{2}} m_B f_\phi\, (m_B A_0^{B\to K^*}, m_\phi F_-^{B\to K^*}, m_\phi F_+^{B\to K^*})$. The estimates above use $F_+^{B\to V_1} = 0.06$ in order to compare with the maximal SM $++$ amplitude. The final state $\bar{K}^*\phi$ does not receive tree contributions. For $\alpha_{1,2}$ and $\alpha^s_{11,12}$, we therefore provide results for the final states in square brackets

	$(\bar{K}^*\phi)^{00}$	$(\bar{K}^*\phi)^{--}$	$(\bar{K}^*\phi)^{++}$
α_1 $[\rho\bar{K}^*]$	$0.987 + 0.021i$	$1.101 + 0.041i$	1.018
α_2 $[\bar{K}^*\rho]$	$0.240 - 0.084i$	$-0.173 - 0.169i$	0.170
α^s_{11} $[\rho\bar{K}^*]$	0	0	0
α^s_{12} $[\bar{K}^*\rho]$	$-0.007 - 0.003i$	-0.002	$-0.247 - 0.068i$
α^u_3	$0.0001 - 0.0005i$	$-0.0023 - 0.0010i$	-0.0035
α^u_4	$-0.026 - 0.015i$	$-0.044 - 0.017i$	-0.031
δP^u_4	1.4×10^{-5}	0.7×10^{-5}	2.2×10^{-5}
δP^u_6	-1.5×10^{-5}	0	0
α'^u_3	$(-0.2 + 1.3i) \times 10^{-5}$	$(5.1 + 2.3i) \times 10^{-6}$	0.0010
α'^u_4	$0.0011 + 0.0006i$	$0.0001 + 5.5 \times 10^{-5} i$	$0.0173 + 0.0074i$
$\delta P'^u_4$	$-0.0005 - 0.0007i$	$-0.0004 - 0.0007i$	$-0.0007 - 0.0007i$
$\delta P'^u_6$	-0.0003	0	0
$\alpha^u_{3,\mathrm{EW}}$	$-0.0084 - 0.0001i$	$0.0044 - 0.0003i$	-0.009
$\alpha^u_{4,\mathrm{EW}}$	$-0.0017 + 0.0007i$	$0.0015 + 0.0014i$	-0.0015
α^u_{3s}	0	0	0
α^u_{4s}	$(9.7 + 3.7i) \times 10^{-5}$	2.0×10^{-5}	$0.0031 + 0.0008i$

Among the Higgs penguin amplitudes α^p_{3q} is the larger of $\alpha^p_{3q,4q}$, since α^p_{4q} is colour-suppressed and is further reduced by the radiative correction given in (33). However, the strong constraint on C^s_{13} renders α^p_{3q} always negligible, in particular as it should be compared to the QCD penguin amplitude α^p_4 rather than the electroweak penguin. This remains true for VP amplitudes despite the fact that the SM penguin amplitude is smaller for these final states, and for PV amplitudes, where α^p_{3q} vanishes.

$B \to VV$

The effect of Higgs exchange is also negligible in case of the longitudinal amplitude in $\bar{B} \to VV$ decays, since it follows the same pattern as for the PV decays with $M_2 = V$. Due to the inverted hierarchy of the transverse polarization amplitudes, see (29), the minus-helicity amplitude is suppressed, while the plus-helicity amplitude is enhanced by a factor of $m_b/\Lambda_{\mathrm{QCD}}$ relative to the SM. To compare the Higgs contributions to the plus-helicity amplitude in the SM, in Table 2

we show the α_i coefficients assuming $F_+^{B\to V_1} = 0.06$, which is the upper limit allowed in [32]. It is evident that the magnitude of the Higgs-induced α_i coefficients is now larger for the plus amplitude than for PP, PV final states and the other polarization amplitudes. In fact, α_{3s}^u would now be comparable to the SM penguin amplitude, if it were not annihilated by the projection on the vector meson at tree level, see (31). Thus, among amplitudes with the same flavour topology, we find that only α_{12}^s is larger than the corresponding SM colour-suppressed tree amplitude α_2. The mirror QCD penguin amplitude $\alpha_4'^u$ amounts to a substantial fraction of the standard penguin amplitude that may reach one if $F_+^{B\to V_1}$ is smaller than the assumed value. This would affect these azimuthal angular distribution of $\Delta S = 1$ decays; in practice, however, these effects are unobservable. Not only are the amplitudes very small in absolute terms, but the tree amplitudes are also subleading to the penguin amplitudes in $\Delta S = 1$ decays.

It is straightforward to compute branching fractions, CP asymmetries and polarization observables including the Higgs-exchange contributions. However, since the α_i parameters discussed above form the basic constituents of observables, it follows that any modification of the SM predictions will be invisible within theoretical uncertainties.

6 Conclusion

Motivated by the interest in the minimally flavour-violating MSSM with large $\tan\beta$ owing to its potentially large impact on leptonic B decays, we analyzed non-leptonic B decays in this model. The hadronic and leptonic flavour-changing interactions are closely related, which allows us to translate the present limit on the $B_s \to \mu^+\mu^-$ branching fraction, and the observation of $B^+ \to \tau^+\nu_\tau$ into a constraint on the Wilson coefficients of the relevant scalar four-quark operators. We then calculated the matrix elements of scalar operators and mirror QCD penguin operators at next-to-leading order in the framework of QCD factorization and find that the limits on leptonic B decay branching fractions exclude any visible effects in hadronic decays, but for an academic exception: the positive-helicity amplitude of $\bar{B} \to VV$ may receive order one modifications relative to the SM, but this amplitude is too small to be detected at present or planned B factories.

Acknowledgements We are grateful to J. Rohrer and De-shan Yang for many discussions and comparisons on QCD factorization results for $B \to VV$ decays. M.B. thanks the CERN Theory group for hospitality. This work is supported by the DFG Sonderforschungsbereich/Transregio 9 "Computergestützte Theoretische Teilchenphysik". X.-Q. Li acknowledges support from the Alexander-von-Humboldt Foundation.

References

1. C. Hamzaoui, M. Pospelov, M. Toharia, Phys. Rev. D **59**, 095005 (1999). hep-ph/9807350
2. K.S. Babu, C.F. Kolda, Phys. Rev. Lett. **84**, 228 (2000). hep-ph/9909476
3. P.H. Chankowski, L. Slawianowska, Phys. Rev. D **63**, 054012 (2001). hep-ph/0008046
4. C.S. Huang, W. Liao, Q.S. Yan, S.H. Zhu, Phys. Rev. D **63**, 114021 (2001) Erratum: Phys. Rev. D **64**, 059902 (2001). hep-ph/0006250
5. C. Bobeth, T. Ewerth, F. Krüger, J. Urban, Phys. Rev. D **64**, 074014 (2001). hep-ph/0104284
6. G. Degrassi, P. Gambino, G.F. Giudice, J. High Energy Phys. **0012**, 009 (2000). hep-ph/0009337
7. M.S. Carena, D. Garcia, U. Nierste, C.E.M. Wagner, Phys. Lett. B **499**, 141 (2001). hep-ph/0010003
8. G. Isidori, A. Retico, J. High Energy Phys. **0111**, 001 (2001). hep-ph/0110121
9. A.J. Buras, P.H. Chankowski, J. Rosiek, L. Slawianowska, Phys. Lett. B **546**, 96 (2002). hep-ph/0207241
10. A.J. Buras, P.H. Chankowski, J. Rosiek, L. Slawianowska, Nucl. Phys. B **659**, 3 (2003). hep-ph/0210145
11. A.G. Akeroyd, S. Recksiegel, J. Phys. G **29**, 2311 (2003). hep-ph/0306037
12. G. Isidori, P. Paradisi, Phys. Lett. B **639**, 499 (2006). hep-ph/0605012
13. U. Nierste, S. Trine, S. Westhoff, Phys. Rev. D **78**, 015006 (2008). arXiv:0801.4938 [hep-ph]
14. J.F. Cheng, C.S. Huang, Phys. Lett. B **554**, 155 (2003). hep-ph/0207177
15. J.F. Cheng, C.S. Huang, X.H. Wu, Phys. Lett. B **585**, 287 (2004). hep-ph/0306086
16. J.F. Cheng, C.S. Huang, X.H. Wu, Nucl. Phys. B **701**, 54 (2004). hep-ph/0404055
17. P.K. Das, K.C. Yang, Phys. Rev. D **71**, 094002 (2005). hep-ph/0412313
18. C.S. Huang, P. Ko, X.H. Wu, Y.D. Yang, Phys. Rev. D **73**, 034026 (2006). hep-ph/0511129
19. J.F. Cheng, Y.N. Gao, C.S. Huang, X.H. Wu, Phys. Lett. B **647**, 413 (2007). hep-ph/0612116
20. Y.L. Wu, C. Zhuang, Phys. Rev. D **75**, 115006 (2007). hep-ph/0701072
21. H. Hatanaka, K.C. Yang, Phys. Rev. D **77**, 035013 (2008). arXiv:0711.3086 [hep-ph]
22. M. Beneke, G. Buchalla, M. Neubert, C.T. Sachrajda, Phys. Rev. Lett. **83**, 1914 (1999). hep-ph/9905312
23. M. Beneke, G. Buchalla, M. Neubert, C.T. Sachrajda, Nucl. Phys. B **591**, 313 (2000). hep-ph/0006124
24. M. Beneke, G. Buchalla, M. Neubert, C.T. Sachrajda, Nucl. Phys. B **606**, 245 (2001). hep-ph/0104110
25. A.J. Buras, M. Misiak, J. Urban, Nucl. Phys. B **586**, 397 (2000). hep-ph/0005183
26. T. Aaltonen et al. (CDF Collaboration), Phys. Rev. Lett. **100**, 101802 (2008). arXiv:0712.1708 [hep-ex]
27. W.S. Hou, Phys. Rev. D **48**, 2342 (1993)
28. E. Barberio et al. (Heavy Flavor Averaging Group), arXiv:0808.1297 [hep-ex]
29. B. Aubert et al. (BABAR Collaboration), Phys. Rev. D **77**, 011107 (2008). arXiv:0708.2260 [hep-ex]
30. Belle Collaboration, arXiv:0809.3834 [hep-ex]
31. M. Beneke, M. Neubert, Nucl. Phys. B **675**, 333 (2003). hep-ph/0308039

32. M. Beneke, J. Rohrer, D. Yang, Nucl. Phys. B **774**, 64 (2007). hep-ph/0612290
33. M. Bauer, B. Stech, M. Wirbel, Z. Phys. C **34**, 103 (1987)
34. M. Beneke, J. Rohrer, D. Yang, Phys. Rev. Lett. **96**, 141801 (2006). hep-ph/0512258
35. H.Y. Cheng, K.C. Yang, Phys. Rev. D **78**, 094001 (2008). arXiv:0805.0329 [hep-ph]
36. M. Beneke, M. Neubert, Nucl. Phys. B **651**, 225 (2003). hep-ph/0210085